# *PVT* and DTA Measurements on trans-4-*n*-Hexyl-(4'-Cyanophenyl)-Cyclohexane (6PCH) up to 300 MPa

M. Sandmann, F. Hamann, and A. Würflinger

Physical Chemistry II, Ruhr University, D-44780 Bochum, Germany

Reprint requests to Prof. A. W., Fax: +49 234 7094 183,
E-mail: Albert.Wuerflinger.ruhr-uni-bochum.de

Z. Naturforsch. **54 a,** 281–286 (1999); received March 13, 1999

The phase diagram of trans-4-*n*-hexyl-(4'-cyanophenyl)-cyclohexane, (6PCH) has been established by high-pressure differential thermal analysis. Specific volumes are presented for temperatures between 300 and 370 K up to 300 MPa. The $p, V_m, T$ data have been determined for the nematic, isotropic, and (partly, in the neighbourhood to the melting curve) solid phases. Volume and enthalpy changes along the phase transitions have also been calculated. As previously, the $p, V_m, T$ data were used to calculate the volume entropy for the nematic-isotropic transition. The molar volumes along the clearing line $T_{\mathrm{NI}}(p)$ enabled us to calculate the molecular field parameter $\gamma = \partial \ln T_{\mathrm{NI}} / \partial \ln V_{\mathrm{NI}}$, being 4.1.

*Key words:* 6PCH; High Pressure; *pVT*; Phase Transitions; Thermodynamics.

## 1. Introduction

Recently we established $p, V_m, T$ data for several liquid crystals belonging to the 4'-*n*-alkyl-biphenyl-4-carbonitrile (*n*CB, $n$ = 5, 6, 7, 8) and trans-4-*n*-alkyl-4'-cyanophenyl-cyclohexane (*n*PCH, $n$ = 8) series [1 - 4]. Comparison of the data for *n*CBs, *n*PCHs, and *n*CCHs shows that the specific volumes vary in a systematic way when the molecular core is changed [5]. In the present study we extend the high-pressure work to 6PCH, employing differential thermal analysis and $p, V_m, T$ measurements. The high-pressure behaviour of 6PCH has so far not been reported in literature.

## 2. Experimental

The high-pressure device for the DTA measurements has been described in [6]. The transition temperatures were recorded with thermocouples and registered on-line with the aid of a personal computer [7]. Usually the phase transitions were observed on heating using rates of 0.5 - 2 K/min [8].

The high-pressure dilatometer was developed for volume measurements on liquids and plastic crystals [9] and was recently improved by Jenau [10] and Sandmann [11]. The molten sample is filled in a cylindrical steel cell which is closed at one end by a moving piston. The displacement of the piston is recorded inductively, from which the volume change of the sample is calculated. In general the measurement is performed along an isotherm on decreasing the pressure. Relating the volume changes to known densities at normal pressure, specific volumes are established in the whole $p, T$ range. Lacking densities at normal pressure are determined with a commercial vibrating-tube densimeter Anton Paar DMA58.

The 6PCH sample (trans-4-*n*-hexyl-(4'-cyanophenyl)-cyclohexane or trans-4-(4'-hexyl-cyclohexyl)-benzonitrile) ($M$ = 269.5 g mol$^{-1}$) was synthesized and purified by Dąbrowski in the Institute of Chemistry, Military Academy of Technology (Warsaw, Poland).

## 3. Results

The phase diagram of 6PCH presented in Fig. 1 was established both by differential thermal analysis and volume measurements. The nematic range of 7 K at normal pressure increases significantly at higher pressures. The melting temperature at normal pressure (315 K) agrees with data from Pohl et al. [12], whilst the clearing temperature (322.4) is 2 K higher. For the odd numbered *n*PCHs the nematic temperature range is considerably larger [12 - 14]. The transi-

0932–0784 / 99 / 0500–0281 $ 06.00 © Verlag der Zeitschrift für Naturforschung, Tübingen · www.znaturforsch.com

Dieses Werk wurde im Jahr 2013 vom Verlag Zeitschrift für Naturforschung in Zusammenarbeit mit der Max-Planck-Gesellschaft zur Förderung der Wissenschaften e.V. digitalisiert und unter folgender Lizenz veröffentlicht: Creative Commons Namensnennung-Keine Bearbeitung 3.0 Deutschland Lizenz.

This work has been digitalized and published in 2013 by Verlag Zeitschrift für Naturforschung in cooperation with the Max Planck Society for the Advancement of Science under a Creative Commons Attribution-NoDerivs 3.0 Germany License.

Zum 01.01.2015 ist eine Anpassung der Lizenzbedingungen (Entfall der Creative Commons Lizenzbedingung „Keine Bearbeitung") beabsichtigt, um eine Nachnutzung auch im Rahmen zukünftiger wissenschaftlicher Nutzungsformen zu ermöglichen.

On 01.01.2015 it is planned to change the License Conditions (the removal of the Creative Commons License condition "no derivative works"). This is to allow reuse in the area of future scientific usage.

Table 1. Specific volumes ($g^{-1} \cdot cm^3$) of 6PCH for the phases Cr, N, and I.

| | — *T*/K — | | | | | | | | | |
|---|---|---|---|---|---|---|---|---|---|---|
| *p*/MPa | 325.15 | 330.15 | 335.15 | 340.15 | 345.15 | 350.15 | 355.15 | 360.15 | 365.15 | 370.15 |
| 0.1 | 1.073 | 1.078 | 1.082 | 1.086 | 1.090 | 1.094 | 1.098 | 1.102 | 1.105 | 1.108 |
| 10 | 1.060 | 1.070 | 1.075 | 1.079 | 1.083 | 1.087 | 1.090 | 1.094 | 1.097 | 1.101 |
| 20 | 1.051 | 1.058 | 1.067 | 1.072 | 1.076 | 1.079 | 1.083 | 1.086 | 1.089 | 1.093 |
| 30 | 1.044 | 1.051 | 1.060 | 1.064 | 1.069 | 1.072 | 1.076 | 1.079 | 1.082 | 1.085 |
| 40 | 0.963 | 1.044 | 1.050 | 1.057 | 1.062 | 1.065 | 1.069 | 1.072 | 1.075 | 1.078 |
| 50 | 0.948 | 1.039 | 1.043 | 1.047 | 1.056 | 1.059 | 1.062 | 1.065 | 1.068 | 1.071 |
| 60 | 0.944 | 0.954 | 1.037 | 1.041 | 1.046 | 1.053 | 1.056 | 1.059 | 1.061 | 1.064 |
| 70 | 0.941 | 0.944 | 1.032 | 1.035 | 1.040 | 1.047 | 1.050 | 1.053 | 1.055 | 1.058 |
| 80 | 0.939 | 0.941 | 0.947 | 1.030 | 1.035 | 1.038 | 1.045 | 1.047 | 1.049 | 1.052 |
| 90 | 0.936 | 0.939 | 0.942 | 1.025 | 1.029 | 1.033 | 1.036 | 1.039 | 1.043 | 1.046 |
| 100 | 0.934 | 0.937 | 0.940 | 0.945 | 1.025 | 1.028 | 1.030 | 1.033 | 1.038 | 1.041 |
| 110 | 0.932 | 0.934 | 0.937 | 0.939 | 1.020 | 1.023 | 1.025 | 1.028 | 1.031 | 1.036 |
| 120 | 0.930 | 0.932 | 0.935 | 0.938 | 0.943 | 1.018 | 1.020 | 1.022 | 1.025 | 1.028 |
| 130 | 0.928 | 0.930 | 0.933 | 0.935 | 0.938 | 1.014 | 1.016 | 1.018 | 1.021 | 1.023 |
| 140 | 0.926 | 0.928 | 0.931 | 0.933 | 0.935 | 0.943 | 1.011 | 1.013 | 1.016 | 1.018 |
| 150 | 0.924 | 0.926 | 0.929 | 0.931 | 0.933 | 0.936 | 1.007 | 1.009 | 1.012 | 1.014 |
| 160 | 0.922 | 0.924 | 0.927 | 0.929 | 0.931 | 0.932 | 0.942 | 1.005 | 1.008 | 1.009 |
| 170 | 0.920 | 0.923 | 0.925 | 0.927 | 0.929 | 0.930 | 0.934 | 1.002 | 1.004 | 1.005 |
| 180 | 0.919 | 0.921 | 0.923 | 0.925 | 0.927 | 0.928 | 0.929 | 0.939 | 1.000 | 1.002 |
| 190 | 0.917 | 0.919 | 0.922 | 0.924 | 0.925 | 0.926 | 0.927 | 0.932 | 0.947 | 0.998 |
| 200 | 0.915 | 0.917 | 0.920 | 0.922 | 0.923 | 0.925 | 0.925 | 0.927 | 0.936 | 0.995 |
| 210 | 0.914 | 0.916 | 0.918 | 0.920 | 0.921 | 0.923 | 0.924 | 0.925 | 0.928 | 0.992 |
| 220 | 0.912 | 0.914 | 0.917 | 0.919 | 0.920 | 0.921 | 0.922 | 0.923 | 0.925 | 0.941 |
| 230 | 0.911 | 0.913 | 0.915 | 0.917 | 0.918 | 0.919 | 0.920 | 0.921 | 0.923 | 0.930 |
| 240 | 0.910 | 0.912 | 0.914 | 0.916 | 0.917 | 0.918 | 0.919 | 0.920 | 0.921 | 0.924 |
| 250 | 0.909 | 0.910 | 0.913 | 0.914 | 0.915 | 0.916 | 0.917 | 0.918 | 0.919 | 0.921 |
| 260 | 0.907 | 0.909 | 0.911 | 0.913 | 0.914 | 0.915 | 0.916 | 0.917 | 0.918 | 0.919 |
| 270 | 0.906 | 0.908 | 0.910 | 0.912 | 0.913 | 0.913 | 0.914 | 0.915 | 0.916 | 0.918 |
| 280 | 0.905 | 0.907 | 0.909 | 0.910 | 0.912 | 0.912 | 0.913 | 0.914 | 0.915 | 0.916 |

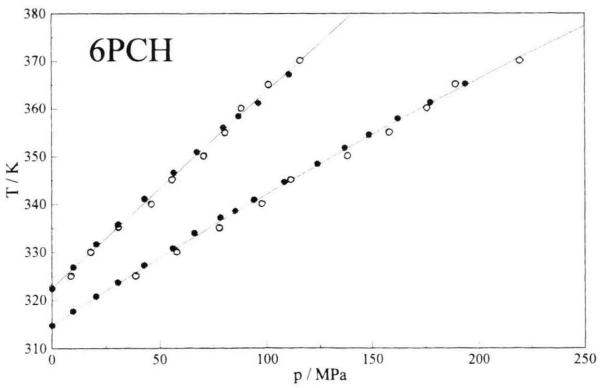


Fig. 1. Phase diagram for 6PCH, (○ $pVT$, • DTA).

tion temperatures have been fitted to polynomials of second order:

$$\text{Cr-N: } T(p)/\text{K} = 314.84 + 0.287\ (p/\text{MPa}) - 1.472 \cdot 10^{-4}\ (p/\text{MPa})^2,$$

$$\text{N-I: } T(p)/\text{K} = 322.54 + 0.417\ (p/\text{MPa}) - 0.576 \cdot 10^{-4}\ (p/\text{MPa})^2.$$

In Fig. 2 the specific volumes are plotted as functions of pressure for different isotherms. The large step in the isotherms comes from the volume change on melting, the small step reflects the nematic-isotropic transition. The isotherms in Fig. 2 show a curvature immediately before the crystal-nematic transition. This pretransitional effect renders the accurate determination of the volume change rather difficult.

The specific volume data are collected in Table 1; a line in a column separates different phases. In Fig. 3 the specific volumes are displayed as functions of temperature in comparison with previous work on various *n*PCHs and *n*CBs [1 - 4, 15]. We note a clear increase in the specific volumes with increasing chain length, both at normal and elevated pressures. Moreover the specific volumes increase when a phenyl ring of the molecular core is replaced by cyclohexyl. Similar trends are observed in the *n*CCH series [5].

The enthalpy and entropy changes accompanying the phase transitions have been evaluated using

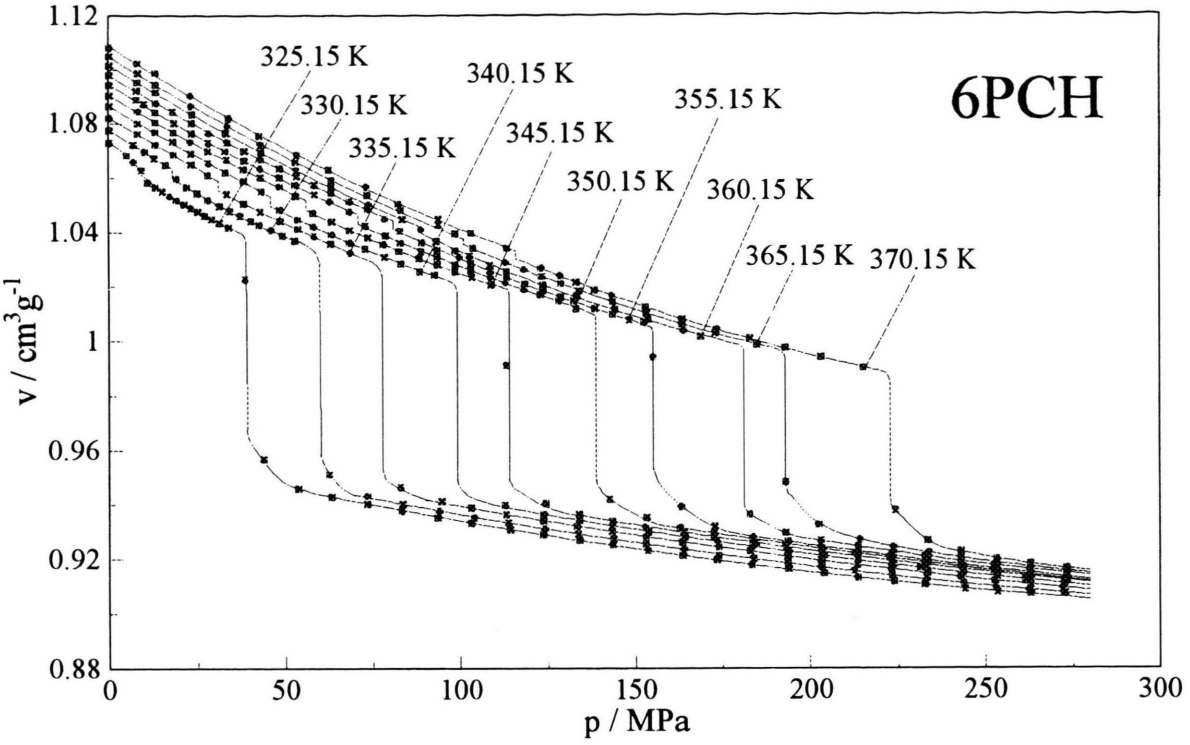


Fig. 2. Specific volumes of 6PCH as functions of pressure; the steps in the isotherms refer to the transitions: cr → nematic, nematic → isotropic.

Table 2. Thermodynamic properties of 6PCH.

| Phase transition | $T$ K | $p$ MPa | $\Delta V_m$ $cm^3 \cdot mol^{-1}$ | $\Delta H_m$ $kJ \cdot mol^{-1}$ | $\Delta S_m$ $J \cdot mol^{-1} \cdot K^{-1}$ |
|---|---|---|---|---|---|
| cr → n | 314.8 | 0.1 | 24.0 | 24.9 | 78.9 |
| | 325.15 | 38.8 | 21.3 | 24.4 | 74.9 |
| | 330.15 | 57.8 | 20.7 | 24.9 | 75.3 |
| | 335.15 | 77.8 | 19.9 | 25.0 | 74.6 |
| | 340.15 | 97.7 | 19.7 | 25.8 | 75.8 |
| | 345.15 | 111.0 | 19.1 | 26.2 | 75.8 |
| | 350.15 | 138.2 | 17.8 | 25.4 | 72.4 |
| | 355.15 | 157.9 | 15.6 | 23.2 | 65.4 |
| | 360.15 | 175.8 | 15.9 | 24.6 | 68.3 |
| | 365.15 | 188.9 | 14.0 | 22.5 | 61.7 |
| | 370.15 | 219.6 | 12.7 | 21.2 | 57.2 |
| n → i | 322.65 | 0.1 | 0.81 | 0.63 | 1.94 |
| | 325.15 | 9.0 | | | |
| | 330.15 | 17.7 | | | |
| | 335.15 | 30.7 | | | |
| | 340.15 | 45.8 | | | |
| | 345.15 | 55.7 | | | |
| | 350.15 | 70.8 | | | |
| | 355.15 | 80.7 | | | |
| | 360.15 | 88.3 | | | |
| | 365.15 | 100.9 | | | |
| | 370.15 | 115.8 | | | |

the Clausius-Clapeyron equation. All thermodynamic quantities are entered in Table 2. Pohl et al. report 28 kJ $mol^{-1}$ for the heat of melting [12], whereas we find 24.9 at atmospheric pressure. The smaller value is partly due to the pretransitional effect. The $\Delta V_{cr-N}$, $\Delta H_{cr-N}$, and $\Delta S_{cr-N}$ values decrease with increasing pressure. For the nematic-isotropic transition no significant pressure dependence of the $\Delta V_{NI}$ and $\Delta H_{NI}$ values can be noted.

## 4. Discussion

As in previous papers, the entropy change at the nematic-isotropic transition, $\Delta S_{NI}$, is splitted into a constant-volume (or configurational) part, and a dilational part [1 - 4]. The latter is calculated with the help of $p, V_m, T$ data: $\Delta S_{dil} = (\partial p/\partial T)_V \Delta V_{NI}$. Combining with standard thermodynamics yields: $\Delta S_{conf}/\Delta S_{NI} = [(\partial p/\partial T)_{NI} - (\partial p/\partial T)_V]/(\partial p/\partial T)_{NI}$, where $\Delta S_{conf} = \Delta S_{NI} - \Delta S_{dil}$ and $(\partial p/\partial T)_{NI}$ is the slope of the NI transition line. $(\partial p/\partial T)_V$ is derived from the slope of isochoric lines close to the clearing temperature, see Figure 4.

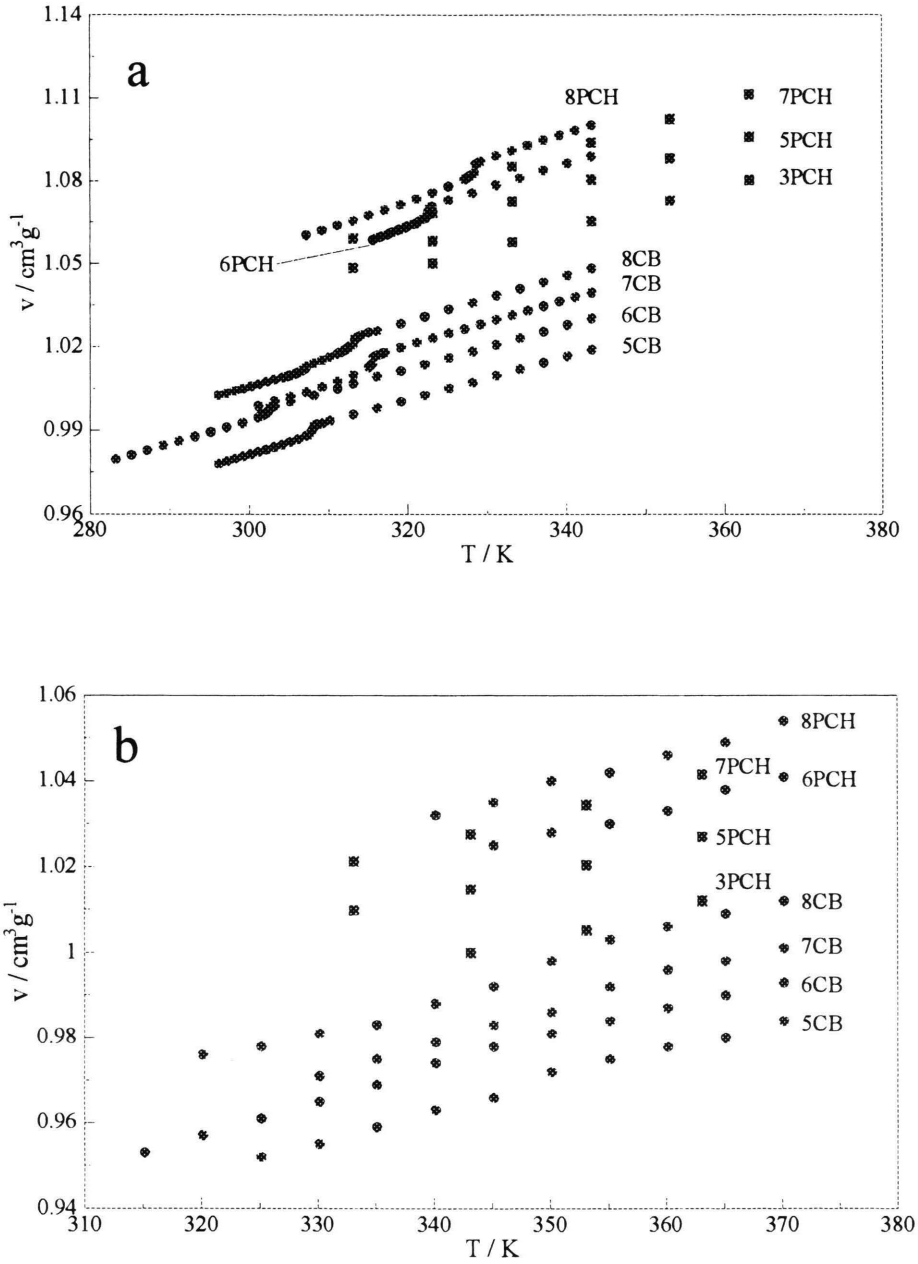


Fig. 3. Specific volumes of *n*CBs and *n*PCHs at a) 1 atm, and b) 100 MPa.

Karasz et al. have heavily questioned the basis and correctness of this entropy separation concept [16], although widely used in literature. The crucial point is that the volume-related entropy increment is not a real state function. The authors [16] have shown that it depends on the path chosen for the intermediate metastable state. Correspondingly $(\partial p/\partial T)_V$ refers either to the low-temperature phase or to the high-temperature phase. In general $(\partial p/\partial T)_V$ of the high-temperature phase is used [17 - 19], in particular for the melting process [20] or order-disorder transitions [21], where $p, V_m, T$ data for the liquid or rotator phase are more readily available. However, it should be born in mind that this entropy separation makes no sense, if $(\partial p/\partial T)_V$ is too different for the high- and low-temperature phases in question.

In the case of the nematic-isotropic transition, Fig. 4 shows that the slopes $(\partial p/\partial T)_V$ are not too dif-

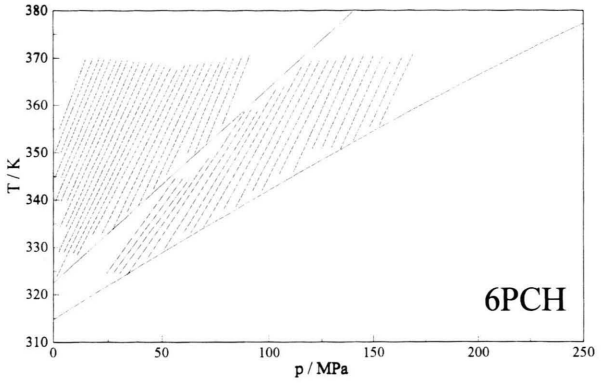


Fig. 4. $T(p)$ diagram for 6PCH with isochores in steps of 0.002 $cm^3g^{-1}$; nematic phase: $v/cm^3g^{-1}$ = 1.004÷1.048, isotropic phase: $v/cm^3g^{-1}$ = 1.046÷1.094.

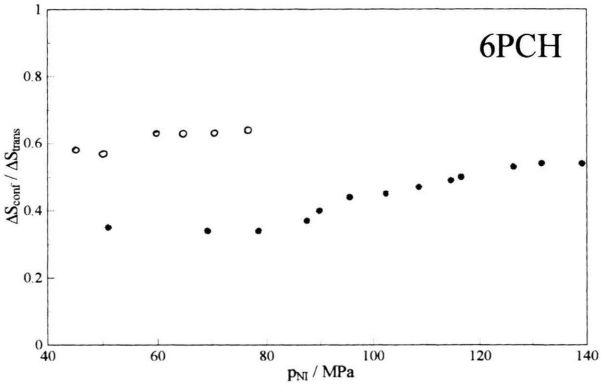


Fig. 5. Entropy separation for the nematic → isotropic transition, using $(\partial p/\partial T)_V$ of the isotropic phase (○) and nematic phase (□).

ferent for the two phases. It was checked for the *n*CBs and *n*PCHs studied [1 - 4] that $(\partial p/\partial T)_V$ changes about ~10÷20 % at the clearing line. In the previous studies [1 - 4] we employed the slopes of the nematic phase, because the temperature range covered in the isotropic phase was generally smaller than the nematic range. In the case of 6PCH the nematic range is unusally small, therefore we use $(\partial p/\partial T)_V$ data for both phases. The result is presented in Fig. 5, showing a ratio $\Delta S_{conf}/\Delta S_{NI} \sim 0.4$ to 0.6, in accordance with previous findings.

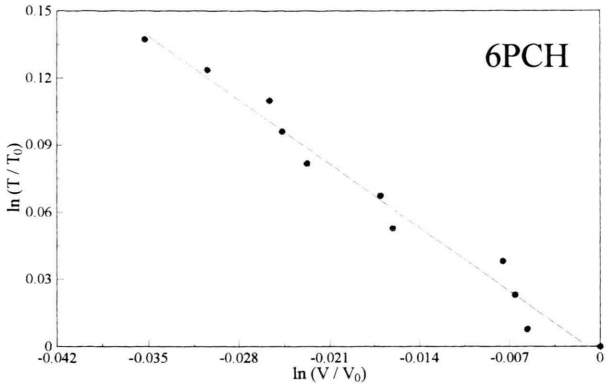


Fig. 6. Logarithm of the clearing temperature against the logarithm of the molar volume for varying pressure, $T_0$ and $V_0$ refer to normal pressure.

Another interesting quantity is the volume dependence of the clearing temperature. The slope $\gamma = \partial \ln T_{NI} / \partial \ln V_{NI}$ is related to the molecular field potential and therefore important for any theoretical discussion of the nematic state. From a corresponding plot (Fig. 6) we derive $\gamma = 4.1$ for 6PCH. In agreement with previous findings, the *n*PCH series yields smaller values for $\gamma$ than the *n*CBs [1 - 5, 22].

*Acknowledgement*

Grants from the Deutsche Forschungsgemeinschaft (Wu 97/10) and Fonds der Chemischen Industrie are gratefully acknowledged.

[1] M. Sandmann, F. Hamann, and A. Würflinger, Z. Naturforsch. **52a**, 739 (1997).

[2] M. Sandmann and A. Würflinger, Z. Naturforsch. **53a**, 233 (1998).

[3] M. Sandmann and A. Würflinger, Z. Naturforsch. **53a**, 787 (1998).

[4] M. Sandmann, D. Büsing, T. Brückert, A. Würflinger, S. Urban, and B. Gestblom, in Proc. SPIE-Int. Soc. Opt. Eng. Vol. **3318** (1998), (Liquid Crystals: Physics, Technology and Applications), 223.

[5] A. Würflinger and M. Sandmann, in: Physical properties of liquid crystals, EMIS Datareview Series, vol. 1: Nematics; Dunmur DA, Fukuda A, Luckhurst GR (eds.), published by the Institution of Electrical Engineers, in press.

[6] A. Würflinger, Ber. Bunsenges. Phys. Chem. **79** (1975) 1195; N. Pingel, U. Poser, and A. Würflinger, J. Chem. Soc. Faraday Trans. I, **80** (1984) 3221.

[7] J. Reuter and A. Würflinger, Ber. Bunsenges. Phys. Chem. **99**, 1247 (1995).

[8] F. Hamann, doctoral thesis, Ruhr-University of Bochum 1998.
[9] R. Landau and A. Würflinger, Rev. Sci. Instrum. **51**, 533 (1980).
[10] M. Jenau, doctoral thesis, Ruhr-University of Bochum 1996.
[11] M. Sandmann, doctoral thesis, Ruhr-University of Bochum 1998.
[12] L. Pohl, R. Eidenschink, J. Krause, and D. Erdmann, Phys. Lett. **60A**, 421 (1977).
[13] S. Urban, B. Gestblom, and A. Würflinger, Mol. Cryst. Liq. Cryst., in press.
[14] P. Kędziora and J. Jadżyn, SPIE **1845**, 333 (1992).
[15] E. Kuss, Mol. Cryst. Liq. Cryst. **76**, 199 (1981).
[16] F. E. Karasz, P. R. Couchman, and D. Klempner, Macromolecules **10**, 88 (1977).
[17] R. A. Orwoll, V. J. Sullivan, and G. C. Campbell, Mol. Cryst. Liq. Cryst. **149**, 121 (1987).
[18] R. G. Horn and T. E. Faber, Proc. R. Soc. A, **368**, 199 (1979); R. G. Horn, J. Phys. Paris **39**, 167 (1978).
[19] A. Abe and S. Y. Nam, Macromolecules **28**, 90 (1995).
[20] A. Würflinger, Colloid Polymer Sci. **262**, 115 (1984).
[21] M. Jenau, J. Reuter, J. Ll. Tamarit, and A. Würflinger, J. Chem. Soc. Faraday Trans. **92**, 1899 (1996); M. Jenau and A. Würflinger, Z. Physik. Chem. (Frankfurt), **199**, 255 (1997).
[22] S. Urban and A. Würflinger, Adv. Chem. Phys. **98**, 143 (1997).